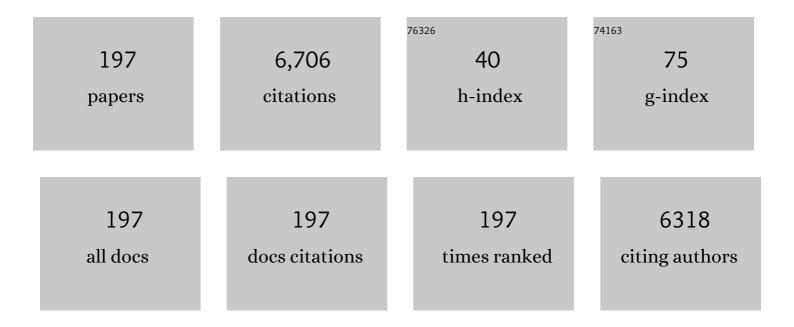
List of Publications by Year in descending order

Source: https://exaly.com/author-pdf/5605693/publications.pdf Version: 2024-02-01



KOU MATSURADA

#	Article	IF	CITATIONS
1	CIGS absorbers and processes. Progress in Photovoltaics: Research and Applications, 2010, 18, 453-466.	8.1	403
2	Terawatt-scale photovoltaics: Transform global energy. Science, 2019, 364, 836-838.	12.6	320
3	Terawatt-scale photovoltaics: Trajectories and challenges. Science, 2017, 356, 141-143.	12.6	303
4	Optical chemical sensor based on surface plasmon measurement. Applied Optics, 1988, 27, 1160.	2.1	297
5	ZnO transparent conducting films deposited by pulsed laser deposition for solar cell applications. Thin Solid Films, 2003, 431-432, 369-372.	1.8	237
6	Uniaxial locked epitaxy of ZnO on the a face of sapphire. Applied Physics Letters, 2000, 77, 1801.	3.3	192
7	Growth of high-quality epitaxial ZnO films on α-Al2O3. Journal of Crystal Growth, 1999, 201-202, 627-632.	1.5	173
8	Nitrogen-induced defects in ZnO:N grown on sapphire substrate by gas source MBE. Journal of Crystal Growth, 2000, 209, 526-531.	1.5	152
9	Interactions between gallium and nitrogen dopants in ZnO films grown by radical-source molecular-beam epitaxy. Applied Physics Letters, 2001, 79, 4139-4141.	3.3	132
10	Band-gap modified Al-doped Zn1â^'xMgxO transparent conducting films deposited by pulsed laser deposition. Applied Physics Letters, 2004, 85, 1374-1376.	3.3	131
11	Polarization-induced two-dimensional electron gases in ZnMgO/ZnO heterostructures. Applied Physics Letters, 2008, 93, .	3.3	131
12	Two-dimensional electron gas in Zn polar ZnMgOâ^•ZnO heterostructures grown by radical source molecular beam epitaxy. Applied Physics Letters, 2006, 89, 132113.	3.3	118
13	ZnO growth on Si by radical source MBE. Journal of Crystal Growth, 2000, 214-215, 50-54.	1.5	116
14	Multilayer system for a high-precision surface plasmon resonance sensor. Optics Letters, 1990, 15, 75.	3.3	111
15	Fabrication of wide-gap Cu(In1â^'xGax)Se2 thin film solar cells: a study on the correlation of cell performance with highly resistive i-ZnO layer thickness. Solar Energy Materials and Solar Cells, 2005, 87, 541-548.	6.2	108
16	Triple-junction thin-film silicon solar cell fabricated on periodically textured substrate with a stabilized efficiency of 13.6%. Applied Physics Letters, 2015, 106, .	3.3	100
17	Ge-incorporated Cu2ZnSnSe4 thin-film solar cells with efficiency greater than 10%. Solar Energy Materials and Solar Cells, 2016, 144, 488-492.	6.2	95
18	Uniaxial locked growth of high-quality epitaxial ZnO films on -Al2O3. Journal of Crystal Growth, 2000, 209, 532-536.	1.5	85

#	Article	IF	CITATIONS
19	Growth of Undoped ZnO Films with Improved Electrical Properties by Radical Source Molecular Beam Epitaxy. Japanese Journal of Applied Physics, 2001, 40, 250-254.	1.5	85
20	A Compact Surface Plasmon Resonance Sensor for Measurement of Water in Process. Applied Spectroscopy, 1988, 42, 1375-1379.	2.2	81
21	Ultra-high stacks of InGaAs/GaAs quantum dots for high efficiency solar cells. Energy and Environmental Science, 2012, 5, 6233.	30.8	75
22	11.0%-Efficient Thin-Film Microcrystalline Silicon Solar Cells With Honeycomb Textured Substrates. IEEE Journal of Photovoltaics, 2014, 4, 1349-1353.	2.5	73
23	Alkali incorporation control in Cu(In,Ga)Se2 thin films using silicate thin layers and applications in enhancing flexible solar cell efficiency. Applied Physics Letters, 2008, 93, .	3.3	71
24	Electrical and optical interconnection for mechanically stacked multi-junction solar cells mediated by metal nanoparticle arrays. Applied Physics Letters, 2012, 101, .	3.3	68
25	Thickness study of Al:ZnO film for application as a window layer in Cu(In1â^xGax)Se2 thin film solar cell. Applied Surface Science, 2011, 257, 4026-4030.	6.1	67
26	Stabilized 14.0%-efficient triple-junction thin-film silicon solar cell. Applied Physics Letters, 2016, 109, .	3.3	67
27	Degenerate layers in epitaxial ZnO films grown on sapphire substrates. Applied Physics Letters, 2004, 84, 4412-4414.	3.3	65
28	Polycrystalline n -ZnO/p -Cu2 O heterojunctions grown by RF-magnetron sputtering. Physica Status Solidi C: Current Topics in Solid State Physics, 2004, 1, 1067-1070.	0.8	63
29	Determination of crystallographic polarity of ZnO layers. Applied Physics Letters, 2005, 87, 141904.	3.3	63
30	Improved External Efficiency InGaN-Based Light-Emitting Diodes with Transparent Conductive Ga-Doped ZnO as p-Electrodes. Japanese Journal of Applied Physics, 2004, 43, L180-L182.	1.5	59
31	In situ diagnostic methods for thin-film fabrication: utilization of heat radiation and light scattering. Progress in Photovoltaics: Research and Applications, 2004, 12, 219-234.	8.1	57
32	Improvement of ZnO TCO film growth for photovoltaic devices by reactive plasma deposition (RPD). Thin Solid Films, 2005, 480-481, 199-203.	1.8	57
33	Strong excitonic transition of Zn1â xMgxO alloy. Applied Physics Letters, 2007, 91, .	3.3	55
34	Growth of N-doped and Ga+N-codoped ZnO films by radical source molecular beam epitaxy. Journal of Crystal Growth, 2002, 237-239, 503-508.	1.5	54
35	Impact of intrinsic amorphous silicon bilayers in silicon heterojunction solar cells. Journal of Applied Physics, 2018, 124, .	2.5	54
36	Development of high-efficiency flexible Cu(In,Ga)Se2 solar cells: A study of alkali doping effects on CIS, CIGS, and CGS using alkali-silicate glass thin layers. Current Applied Physics, 2010, 10, S154-S156.	2.4	53

#	Article	IF	CITATIONS
37	Room-temperature deposition of Al-doped ZnO films by oxygen radical-assisted pulsed laser deposition. Thin Solid Films, 2002, 422, 176-179.	1.8	52
38	Photoluminescence characterization of Zn1â^'xMgxO epitaxial thin films grown on ZnO by radical source molecular beam epitaxy. Applied Physics Letters, 2007, 90, 124104.	3.3	49
39	Potential of very thin and highâ€efficiency silicon heterojunction solar cells. Progress in Photovoltaics: Research and Applications, 2019, 27, 1061-1070.	8.1	47
40	Negative thermal quenching of photoluminescence in ZnO. Physica B: Condensed Matter, 2006, 376-377, 711-714.	2.7	46
41	Improvement of Electrical Properties in ZnO Thin Films Grown by Radical Source(RS)-MBE. Physica Status Solidi A, 2000, 180, 287-292.	1.7	41
42	Progress and limitations of thin-film silicon solar cells. Solar Energy, 2018, 170, 486-498.	6.1	41
43	Epitaxial growth of ZnO thin films on LiNbO3 substrates. Thin Solid Films, 1999, 347, 238-240.	1.8	40
44	Effect of Se/(Ga+In) ratio on MBE grown Cu(In,Ga)Se2 thin film solar cell. Journal of Crystal Growth, 2009, 311, 2212-2214.	1.5	40
45	Double-sided TOPCon solar cells on textured wafer with ALD SiOx layer. Solar Energy Materials and Solar Cells, 2020, 207, 110357.	6.2	39
46	Effect of band offset on the open circuit voltage of heterojunction CuIn1â^'xGaxSe2 solar cells. Applied Physics Letters, 2004, 85, 5607-5609.	3.3	38
47	Thin-film microcrystalline silicon solar cells: 11.9% efficiency and beyond. Applied Physics Express, 2018, 11, 022301.	2.4	38
48	A silicon nanocrystal/polymer nanocomposite as a down-conversion layer in organic and hybrid solar cells. Nanoscale, 2015, 7, 11566-11574.	5.6	37
49	Palladium nanoparticle array-mediated semiconductor bonding that enables high-efficiency multi-junction solar cells. Japanese Journal of Applied Physics, 2016, 55, 025001.	1.5	37
50	Passivation property of ultrathin SiOx:H / a-Si:H stack layers for solar cell applications. Solar Energy Materials and Solar Cells, 2018, 185, 8-15.	6.2	37
51	Growth and characterization of undoped ZnO films for single crystal based device use by radical source molecular beam epitaxy (RS-MBE). Journal of Crystal Growth, 2001, 227-228, 923-928.	1.5	35
52	Characterization of Zn1â^'xMgxO transparent conducting thin films fabricated by multi-cathode RF-magnetron sputtering. Thin Solid Films, 2010, 518, 2949-2952.	1.8	34
53	Dependence of Se beam pressure on defect states in CIGS-based solar cells. Solar Energy Materials and Solar Cells, 2011, 95, 227-230.	6.2	34
54	The effects of thermal treatments on the electrical properties of phosphorus doped ZnO layers grown by MBE. Journal of Crystal Growth, 2005, 278, 268-272.	1.5	33

#	Article	IF	CITATIONS
55	High electron mobility Zn polar ZnMgO/ZnO heterostructures grown by molecular beam epitaxy. Journal of Crystal Growth, 2007, 301-302, 358-361.	1.5	33
56	Temperature dependence of photocapacitance spectrum of CIGS thin-film solar cell. Thin Solid Films, 2009, 517, 2403-2406.	1.8	33
57	Growth of ZnO and device applications. Applied Surface Science, 2005, 244, 504-510.	6.1	32
58	Progress in the Efficiency of Wide-Gap Cu(In1-xGax)Se2Solar Cells Using CIGSe Layers Grown in Water Vapor. Japanese Journal of Applied Physics, 2005, 44, L679-L682.	1.5	32
59	Band profiles of ZnMgO/ZnO heterostructures confirmed by Kelvin probe force microscopy. Applied Physics Letters, 2009, 94, .	3.3	32
60	InGaP-based InGaAs quantum dot solar cells with GaAs spacer layer fabricated using solid-source molecular beam epitaxy. Applied Physics Letters, 2012, 101, .	3.3	32
61	Characterization of electronic structure of Cu2ZnSn(S Se1â^')4 absorber layer and CdS/Cu2ZnSn(S) Tj ETQq1 2015, 582, 166-170.	1 0.784314 1.8	rgBT /Overloo 31
62	Properties of CuInGaSe2 solar cells based upon an improved three-stage process. Thin Solid Films, 2003, 431-432, 6-10.	1.8	30
63	Plasma-Induced Electronic Defects: Generation and Annihilation Kinetics in Hydrogenated Amorphous Silicon. Physical Review Applied, 2018, 10, .	3.8	30
64	Growth of polycrystalline Cu(In,Ga)Se2 thin films using a radio frequency-cracked Se-radical beam source and application for photovoltaic devices. Applied Physics Letters, 2007, 91, .	3.3	29
65	InGaP solar cells fabricated using solid-source molecular beam epitaxy. Journal of Crystal Growth, 2013, 378, 576-578.	1.5	27
66	On the interplay of cell thickness and optimum period of silicon thinâ€film solar cells: light trapping and plasmonic losses. Progress in Photovoltaics: Research and Applications, 2016, 24, 379-388.	8.1	27
67	Dramatic Enhancement of Photoluminescence Quantum Yields for Surfaceâ€Engineered Si Nanocrystals within the Solar Spectrum. Advanced Functional Materials, 2013, 23, 6051-6058.	14.9	26
68	Impact of silicon wafer thickness on photovoltaic performance of crystalline silicon heterojunction solar cells. Japanese Journal of Applied Physics, 2018, 57, 08RB10.	1.5	26
69	An EXAFS and XANES study of MBE grown Cu-doped ZnO. Nuclear Instruments & Methods in Physics Research B, 2003, 199, 190-194.	1.4	25
70	Effects of Mo back contact thickness on the properties of CIGS solar cells. Physica Status Solidi (A) Applications and Materials Science, 2009, 206, 1063-1066.	1.8	25
71	Development of high-efficiency CIGS integrated submodules using in-line deposition technology. Solar Energy Materials and Solar Cells, 2011, 95, 254-256.	6.2	25
72	Highly Controlled Codeposition Rate of Organolead Halide Perovskite by Laser Evaporation Method. ACS Applied Materials & Interfaces, 2016, 8, 26013-26018.	8.0	25

#	Article	IF	CITATIONS
73	Time-Resolved Microphotoluminescence Study of Cu(In,Ga)Se <sub>2</sub> . Japanese Journal of Applied Physics, 2011, 50, 05FC01.	1.5	25
74	Effects of annealing under various atmospheres on electrical properties of Cu(In,Ga)Se2 films and CdS/Cu(In,Ga)Se2 heterostructures. Thin Solid Films, 2008, 516, 7036-7040.	1.8	24
75	Large grain Cu(In,Ca)Se2 thin film growth using a Se-radical beam source. Solar Energy Materials and Solar Cells, 2009, 93, 792-796.	6.2	24
76	Tunnel current through a miniband in InGaAs quantum dot superlattice solar cells. Solar Energy Materials and Solar Cells, 2011, 95, 2920-2923.	6.2	24
77	Molecular beam epitaxial growth and characterization of CuInSe2 and CuGaSe2 for device applications. Journal of Crystal Growth, 2002, 237-239, 1993-1999.	1.5	23
78	Environmentally Friendly Processing Technology for Engineering Silicon Nanocrystals in Water with Laser Pulses. Journal of Physical Chemistry C, 2016, 120, 18822-18830.	3.1	23
79	Band Alignment of the CdS/Cu <sub>2</sub> Zn(Sn <sub>1â€"<i>x</i></sub> Ge <i>sub&gt;x</i> )Se <sub>4</sub> Heterointerface and Electronic Properties at the Cu <sub>2</sub> Zn(Sn <sub>1â€"<i>x</i></sub> Ge <i>sub&gt;x</i> )Se <sub>4</sub> Surface: <i>x</i>	8.0	23
80	Characterization of ZnO crystals by photoluminescence spectroscopy. Physica Status Solidi C: Current Topics in Solid State Physics, 2004, 1, 872-875.	0.8	22
81	Photoluminescence characterization of excitonic centers in ZnO epitaxial films. Applied Physics Letters, 2005, 86, 221907.	3.3	22
82	Simultaneous measurement of the velocity and the displacement of the moving rough surface by a laser Doppler velocimeter. Applied Optics, 1997, 36, 4516.	2.1	21
83	Nucleation and growth of ZnO on sapphire substrates using molecular beam epitaxy. Journal of Crystal Growth, 2001, 227-228, 911-916.	1.5	21
84	Composition control of Cu2ZnSnSe4-based solar cells grown by coevaporation. Thin Solid Films, 2014, 551, 27-31.	1.8	21
85	Narrow-bandgap Cu2Sn1â^'xGexSe3 thin film solar cells. Materials Letters, 2015, 158, 205-207.	2.6	21
86	On the interplay of interface morphology and microstructure of high-efficiency microcrystalline silicon solar cells. Solar Energy Materials and Solar Cells, 2016, 151, 81-88.	6.2	21
87	Observation of Exciton-Polariton Emissions from a ZnO Epitaxial Film on the a-Face of Sapphire Grown by Radical-Source Molecular-Beam-Epitaxy. Japanese Journal of Applied Physics, 2002, 41, L935-L937.	1.5	19
88	In situ deposition rate monitoring during the three-stage-growth process of Cu(In,Ga)Se2 absorber films. Thin Solid Films, 2003, 431-432, 16-21.	1.8	18
89	Impact of Cu/III ratio on the near-surface defects in polycrystalline CuGaSe2 thin films. Applied Physics Letters, 2011, 98, 112105.	3.3	18
90	Time-Resolved Microphotoluminescence Study of Cu(In,Ga)Se <sub>2</sub> . Japanese Journal of Applied Physics, 2011, 50, 05FC01.	1.5	18

#	Article	IF	CITATIONS
91	InGaAs quantum dot superlattice with vertically coupled states in InGaP matrix. Journal of Applied Physics, 2013, 114, .	2.5	17
92	In(Ga)As quantum dots on InGaP layers grown by solid-source molecular beam epitaxy. Journal of Crystal Growth, 2013, 378, 430-434.	1.5	17
93	InGaP/GaAs tandem solar cells fabricated using solid-source molecular beam epitaxy. Japanese Journal of Applied Physics, 2014, 53, 05FV06.	1.5	17
94	Electronic properties of ultrathin hydrogenated amorphous silicon. Applied Physics Express, 2017, 10, 081401.	2.4	17
95	Effect of Combined Alkali (KF + CsF) Postâ€Deposition Treatment on Cu(InGa)Se <sub>2</sub> Solar Ce Physica Status Solidi - Rapid Research Letters, 2018, 12, 1800372.	llş. 2.4	17
96	Impact of band tail distribution on carrier trapping in hydrogenated amorphous silicon for solar cell applications. Journal of Non-Crystalline Solids, 2016, 436, 44-50.	3.1	16
97	In-situ detection of interface defects in a-Si:H/c-Si heterojunction during plasma processing. Applied Physics Express, 2019, 12, 051006.	2.4	16
98	Growth of LiNbO 3 epitaxial films by oxygen radical-assisted laser molecular beam epitaxy. Applied Physics A: Materials Science and Processing, 1999, 69, S679-S681.	2.3	15
99	Determination of Cu(In1â^'xGax)3Se5 defect phase in MBE grown Cu(In1â^'xGax)Se2 thin film by Rietveld analysis. Solar Energy Materials and Solar Cells, 2011, 95, 231-234.	6.2	15
100	Impact of Se flux on the defect formation in polycrystalline Cu(In,Ga)Se2 thin films grown by three stage evaporation process. Journal of Applied Physics, 2013, 113, 064907.	2.5	15
101	Highly Efficient Cu(In,Ga)Se <sub>2</sub> Thin-Film Submodule Fabricated Using a Three-Stage Process. Applied Physics Express, 2013, 6, 112303.	2.4	15
102	High-quality SiGe films grown with compositionally graded buffer layers for solar cell applications. Journal of Crystal Growth, 2013, 378, 226-229.	1.5	15
103	Fabrication of hydrogenated amorphous Si/crystalline Si <sub>1â^'</sub> <i><sub>x</sub></i> Ge <i><sub>x</sub></i> (i>( <i>x</i> ≤0.84) heterojunction solar cells grown by solid source molecular beam epitaxy. Japanese Journal of Applied Physics, 2015, 54, 012301.	1.5	15
104	Bandgap Engineering in OHâ€Functionalized Silicon Nanocrystals: Interplay between Surface Functionalization and Quantum Confinement. Advanced Functional Materials, 2017, 27, 1701898.	14.9	15
105	Transmission electron microscopy study of GalnNAs(Sb) thin films grown by atomic hydrogen-assisted molecular beam epitaxy. Applied Physics Letters, 2011, 99, 191907.	3.3	14
106	Enhancement of hybrid solar cell performance by polythieno [3,4-b]thiophenebenzodithiophene and microplasma-induced surface engineering of silicon nanocrystals. Applied Physics Letters, 2012, 100, .	3.3	14
107	Highâ€efficiency CIGS submodules. Progress in Photovoltaics: Research and Applications, 2012, 20, 595-599.	8.1	14
108	Change in the electrical performance of GaAs solar cells with InGaAs quantum dot layers by electron irradiation. Solar Energy Materials and Solar Cells, 2013, 108, 263-268.	6.2	14

#	Article	IF	CITATIONS
109	Enhanced efficiency of ultrathin (â^1⁄4500 nm)-film microcrystalline silicon photonic crystal solar cells. Applied Physics Express, 2017, 10, 012302.	2.4	14
110	Effect of thermal annealing on the redistribution of alkali metals in Cu(In,Ga)Se2solar cells on glass substrate. Journal of Applied Physics, 2018, 123, 093101.	2.5	14
111	InGaN-based light-emitting diodes fabricated with transparent Ga-doped ZnO as ohmicp-contact. Physica Status Solidi A, 2004, 201, 2704-2707.	1.7	13
112	Analysis of bulk and interface defects in hydrogenated amorphous silicon solar cells by Fourier transform photocurrent spectroscopy. Journal of Applied Physics, 2015, 118, .	2.5	13
113	Adjusting the sodium diffusion into CuInGaSe2 absorbers by preheating of Mo/SLG substrates. Journal of Physics and Chemistry of Solids, 2003, 64, 1877-1880.	4.0	12
114	Roles of hydrogen atoms in p-type Poly-Si/SiO <i>x</i> passivation layer for crystalline silicon solar cell applications. Japanese Journal of Applied Physics, 2019, 58, 050915.	1.5	12
115	Analysis of Y-branching optical circulator using magnetooptic medium as a substrate. Journal of Lightwave Technology, 1991, 9, 1061-1067.	4.6	11
116	Control of the thin film properties of Cu(In,Ga)Se2 using water vapor introduction during growth. Journal of Applied Physics, 2006, 100, 096106.	2.5	11
117	Key Points in the Latest Developments of Highâ€Efficiency Thinâ€Film Silicon Solar Cells. Physica Status Solidi (A) Applications and Materials Science, 2017, 214, 1700544.	1.8	11
118	Stable ultrathin surfactantâ€free surfaceâ€engineered silicon nanocrystal solar cells deposited at room temperature. Energy Science and Engineering, 2017, 5, 184-193.	4.0	11
119	CIGS solar cell with CdS buffer layer deposited by ammoniaâ€free process. Physica Status Solidi (A) Applications and Materials Science, 2009, 206, 1072-1075.	1.8	10
120	Over 20% Efficiency Mechanically Stacked Multi-Junction Solar Cells Fabricated by Advanced Bonding Using Conductive Nanoparticle Alignments. Materials Research Society Symposia Proceedings, 2013, 1538, 167-171.	0.1	10
121	Growth of InGaAsP solar cells and their application to triple-junction top cells used in smart stack multijunction solar cells. Journal of Vacuum Science and Technology B:Nanotechnology and Microelectronics, 2017, 35, .	1.2	10
122	Effects of low temperature buffer layer treatments on the growth of high quality ZnO films. Physica Status Solidi C: Current Topics in Solid State Physics, 2004, 1, 888-891.	0.8	9
123	Built-In Charges and Photoluminescence Stability of 3D Surface-Engineered Silicon Nanocrystals by a Nanosecond Laser and a Direct Current Microplasma. Journal of Physical Chemistry C, 2013, 117, 10939-10948.	3.1	9
124	Characterization of electronic structure of oxysulfide buffers and band alignment at buffer/absorber interfaces in Cu(In,Ga)Se <sub>2</sub> -based solar cells. Japanese Journal of Applied Physics, 2014, 53, 05FW09.	1.5	9
125	Effect of Front TCO Layer on Properties of Substrate-Type Thin-Film Microcrystalline Silicon Solar Cells. IEEE Journal of Photovoltaics, 2015, 5, 1528-1533.	2.5	9
126	Light absorption enhancement in thin-film GaAs solar cells with flattened light scattering substrates. Journal of Applied Physics, 2017, 122, .	2.5	9

#	Article	IF	CITATIONS
127	Reduced recombination in a surface-sulfurized Cu(InGa)Se <sub>2</sub> thin-film solar cell. Japanese Journal of Applied Physics, 2018, 57, 055701.	1.5	9
128	Formation of electronic defects in crystalline silicon during hydrogen plasma treatment. AIP Advances, 2019, 9, 045110.	1.3	9
129	Electronic structure of Cu <sub>2</sub> ZnSn(S <sub><i>x</i></sub> Se <sub>1â<sup>^</sup><i>x</i></sub> ) <sub>4</sub> surface and CdS/Cu <sub>2</sub> ZnSn(S <sub><i>x</i></sub> Se <sub>1â<sup>^</sup><i>x</i></sub> ) <sub>4</sub> interface. Physica Status Solidi C: Current Topics in Solid State Physics. 2017. 14.	0.8	9
130	Cu-dependent phase transition in polycrystalline CuGaSe2 thin films grown by three-stage process. Journal of Applied Physics, 2011, 110, 014903.	2.5	8
131	Capturing by self-assembled block copolymer thin films: transfer printing of metal nanostructures on textured surfaces. Chemical Communications, 2014, 50, 362-364.	4.1	8
132	Photoreflectance and Photoluminescence of Exciton-Polaritons in a ZnO Epilayer Grown on the a-Face of Sapphire by Radical-Source Molecular-Beam Epitaxy. Physica Status Solidi A, 2002, 192, 171-176.	1.7	7
133	Built-in Potential and Open Circuit Voltage of Heterojunction Culn <sub>1-x</sub> GaxSe <sub>2</sub> Solar Cells. Materials Research Society Symposia Proceedings, 2005, 865, 5191.	0.1	7
134	Optical and structural studies of highly uniform Ge quantum dots on Si (001) substrate grown by solid-source molecular beam epitaxy. Journal of Crystal Growth, 2013, 378, 439-441.	1.5	7
135	Transfer-printed silver nanodisks for plasmonic light trapping in hydrogenated microcrystalline silicon solar cells. Applied Physics Express, 2014, 7, 112302.	2.4	7
136	Effect of pre-annealing on Cu2ZnSnSe4 thin-film solar cells prepared from stacked Zn/Cu/Sn metal precursors. Materials Letters, 2016, 176, 78-82.	2.6	7
137	Electronic structures of Cu <sub>2</sub> ZnSnSe <sub>4</sub> surface and CdS/Cu <sub>2</sub> ZnSnSe <sub>4</sub> heterointerface. Japanese Journal of Applied Physics, 2017, 56, 065701.	1.5	7
138	Structural changes of CIGS during deposition investigated by spectroscopic light scattering: A study on Ga concentration and Se pressure. Solar Energy Materials and Solar Cells, 2006, 90, 3377-3384.	6.2	6
139	Study of Band Alignment at CBD-CdS/Cu(In <sub>1-<i>x</i></sub> Ga <sub><i>x</i></sub> )Se <sub>2</sub> ( <i>x</i> = 0.2 - 1.0) Interfaces by Photoemission and Inverse Photoemission Spectroscopy. Materials Research Society Symposia Proceedings, 2007, 1012, 1.	0.1	6
140	Investigation of relation between Ga concentration and defect levels of Al/Cu(In,Ga)Se2 Schottky junctions using admittance spectroscopy. Thin Solid Films, 2007, 515, 6208-6211.	1.8	6
141	Efficiency limit analysis of organic solar cells: model simulation based on vanadyl phthalocyanine/C60planar junction cell. Japanese Journal of Applied Physics, 2014, 53, 01AB12.	1.5	6
142	Structural influences on charge carrier dynamics for small-molecule organic photovoltaics. Journal of Applied Physics, 2014, 116, 013105.	2.5	6
143	Investigation of InGaP/(In)AlGaAs/GaAs triple-junction top cells for smart stacked multijunction solar cells grown using molecular beam epitaxy. Japanese Journal of Applied Physics, 2015, 54, 08KE02.	1.5	6
144	Natural ordering of ZnO1â^'xSex grown by radical source MBE. Journal of Crystal Growth, 2003, 251, 633-637.	1.5	5

#	Article	IF	CITATIONS
145	The chemical environment about Cd atoms in Cd chemical bath treated CuInSe2 and CuGaSe2. Journal of Physics and Chemistry of Solids, 2003, 64, 1733-1735.	4.0	5
146	Determination of crystallographic polarity of ZnO bulk crystals and epilayers. Physica Status Solidi C: Current Topics in Solid State Physics, 2006, 3, 1018-1021.	0.8	5
147	Local Structure around Dopant Site in Ga-Doped ZnO from Extended X-ray Absorption Fine Structure Measurements. Journal of the Physical Society of Japan, 2011, 80, 074602.	1.6	5
148	Highly efficient and reliable mechanically stacked multi-junction solar cells using advanced bonding method with conductive nanoparticle alignments. , 2014, , .		5
149	MBE-grown InGaAsP solar cells with 1.0 eV bandgap on InP(001) substrates for application to multijunction solar cells. Japanese Journal of Applied Physics, 2015, 54, 08KE10.	1.5	5
150	Tiling of Solar Cell Surfaces: Influence on Photon Management and Microstructure. Advanced Materials Interfaces, 2018, 5, 1700814.	3.7	5
151	Observation of Interdiffusion in ZnO/CuInSe2 Heterostructures and its Effect on Film Properties. Materials Research Society Symposia Proceedings, 2001, 668, 1.	0.1	4
152	A Study of the Diffusion and pn-Junction Formation in CIGS Solar Cells using EBIC and EDX Measurements. Materials Research Society Symposia Proceedings, 2005, 865, 631.	0.1	4
153	Effects of water vapor introduction during Cu(In1-xGax)Se2deposition on thin film properties and solar cell performance. Physica Status Solidi (A) Applications and Materials Science, 2006, 203, 2609-2614.	1.8	4
154	Light Trapping by Ag Nanoparticles Chemically Assembled inside Thin-Film Hydrogenated Microcrystalline Si Solar Cells. Japanese Journal of Applied Physics, 2012, 51, 042302.	1.5	4
155	Control of Optical and Electrical Properties of ZnO Films for Photovoltaic Applications. Materials Research Society Symposia Proceedings, 2001, 668, 1.	0.1	3
156	Point Defect Changes in CuGaSe2 Induced by Gas Annealing. Materials Research Society Symposia Proceedings, 2003, 763, 5171.	0.1	3
157	Integration of Surfactant-Free Silicon Nanocrystal in Hybrid Solar Cells. Japanese Journal of Applied Physics, 2012, 51, 10NE25.	1.5	3
158	Electrical performance degradation of GaAs solar cells with InGaAs quantum dot layers due to proton irradiation. , 2013, , .		3
159	Band Alignment of CdS/Cu2ZnSnSe4 Heterointerface and Solar Cell Performances. MRS Advances, 2017, 2, 3157-3162.	0.9	3
160	Role of the Fermi level in the formation of electronic band-tails and mid-gap states of hydrogenated amorphous silicon in thin-film solar cells. Journal of Applied Physics, 2017, 122, 093101.	2.5	3
161	Hydrogen-induced defects in crystalline silicon during growth of an ultrathin a-Si:H layer. Japanese Journal of Applied Physics, 2020, 59, SHHE05.	1.5	3
162	Y-Branch TE-TM Mode Splitter Using Multilayered Waveguide. Japanese Journal of Applied Physics, 1992, 31, 1636-1640.	1.5	2

#	Article	IF	CITATIONS
163	Significant Compositional Changes and Formation of a Ga-O Phase after Oxygen-annealing of Ga-rich CuGaSe <sub>2</sub> Films. Materials Research Society Symposia Proceedings, 2001, 668, 1.	0.1	2
164	Structural changes of CuGaSe2 films during the three-stage process observed by spectroscopic light scattering. Thin Solid Films, 2005, 480-481, 367-372.	1.8	2
165	Study on electrical properties of Al/Cu(In,Ca)Se2 Schottky junction and ZnO/CdS/Cu(In,Ca)Se2 heterojunction using admittance spectroscopy. Physica Status Solidi C: Current Topics in Solid State Physics, 2006, 3, 2576-2580.	0.8	2
166	<i>In-situ</i> Characterization of As-grown Surface of CIGS Films. Materials Research Society Symposia Proceedings, 2007, 1012, 1.	0.1	2
167	Correlation between Electrical Properties and Crystal c-Axis Orientation of Zinc Oxide Transparent Conducting Films. Japanese Journal of Applied Physics, 2012, 51, 10NC16.	1.5	2
168	Miniband formation in InGaAs quantum dot superlattice with InGaP matrix for application to intermediate-band solar cells. , 2013, , .		2
169	Observation of Sodium Diffusion in CIGS Solar Cells with Mo/TCO/Mo Hybrid Back Contacts. Materials Research Society Symposia Proceedings, 2013, 1538, 61-66.	0.1	2
170	Radiation response of the fill-factor for GaAs solar cells with InGaAs quantum dot layers. , 2014, , .		2
171	Effect of deposition rate on the characteristics of Ge quantum dots on Si (001) substrates. Thin Solid Films, 2014, 557, 80-83.	1.8	2
172	MBE-grown InGaP/GaAs/InGaAsP triple junction solar cells fabricated by advanced bonding technique. , 2014, , .		2
173	Electrical characteristics of amorphous Si:H/crystalline Si0.3Ge0.7 heterojunction solar cells grown on compositionally graded buffer layers. Journal of Crystal Growth, 2015, 425, 162-166.	1.5	2
174	Reduced potential fluctuation in a surface sulfurized Cu(InGa)Se2. Japanese Journal of Applied Physics, 2018, 57, 085702.	1.5	2
175	Silicon Thin-Film Solar Cells Approaching the Geometric Light-Trapping Limit: Surface Texture Inspired by Self-Assembly Processes. ACS Photonics, 2018, 5, 2799-2806.	6.6	2
176	Hydrogen passivation effect on p-type poly-Si/SiOx stack for crystalline silicon solar cells. AIP Conference Proceedings, 2019, , .	0.4	2
177	Fabrication and Characterization of Cu(In,Ga)(S,Se)2-Based Solar Cells. Japanese Journal of Applied Physics, 2012, 51, 10NC04.	1.5	2
178	Influence of interstripe gain on crosscoupled-mode operation in twin-stripe lasers. IEEE Journal of Quantum Electronics, 1993, 29, 2855-2858.	1.9	1
179	Fabrication and Characterization of Wide-Gap ZnCuInS\$_{2}\$ Solar Cells. Japanese Journal of Applied Physics, 2012, 51, 10NC06.	1.5	1
180	Fabrication and Characterization of Cu(In,Ga)(S,Se)\$_{2}\$-Based Solar Cells. Japanese Journal of Applied Physics, 2012, 51, 10NC04.	1.5	1

#	ARTICLE	IF	CITATIONS
181	Enhancement of polymer solar cell performance under low-concentrated sunlight by 3D surface-engineered silicon nanocrystals. , 2013, , .		1
182	Compositional dependence photoluminescence study of polycrystalline CuGaSe2 thin films. , 2015, , .		1
183	Impact of front TCO layer in substrate-type thin-film microcrystalline silicon solar cells. , 2015, , .		1
184	Improvement of In2 S3 /ZnCuInS2 interfaces for wide-gap solar cells. Physica Status Solidi C: Current Topics in Solid State Physics, 2015, 12, 769-772.	0.8	1
185	Strain-compensated Ge/Si1â~'C quantum dots with Si mediating layers grown by molecular beam epitaxy. Journal of Crystal Growth, 2015, 425, 167-171.	1.5	1
186	Impact of carrier doping on electrical properties of laser-induced liquid-phase-crystallized silicon thin films for solar cell application. Japanese Journal of Applied Physics, 2018, 57, 021302.	1.5	1
187	Thermal processing induced structural changes in ZnO films grown on (11&2macr;0) sapphire substrates using molecular beam epitaxy. Physica Status Solidi C: Current Topics in Solid State Physics, 2004, 1, 868-871.	0.8	0
188	XAFS Observations of Initial Growth of 0001 ZnO on Sapphire Substrates. Physica Scripta, 2005, , 523.	2.5	0
189	Photoluminescence recombination centers in ZnO. Physica Status Solidi C: Current Topics in Solid State Physics, 2006, 3, 1026-1029.	0.8	0
190	Formation of two-dimensional electron gas and enhancement of electron mobility by Zn polar ZnMgO/ZnO heterostructures. , 2007, 6474, 78.		0
191	Study of Band Alignment at the Interface between CBD-CdS and CIGS grown by H2O-introduced co-evaporation. Materials Research Society Symposia Proceedings, 2007, 1012, 1.	0.1	0
192	Fabrication of 0.9 eV bandgap a-Si/c-Si <inf>1−x</inf> Ge <inf>x</inf> heterojunction solar cells. , 2014, , .		0
193	Surface-engineered silicon nanocrystals as high energy photons downshifters for organic and hybrid solar cells. , 2014, , .		0
194	Integration of Light Trapping Silver Nanostructures in Hydrogenated Microcrystalline Silicon Solar Cells by Transfer Printing. Journal of Visualized Experiments, 2015, , e53276.	0.3	0
195	Wide-gap solar cells using a novel ZnCuGaSe <sub>2</sub> absorber. Japanese Journal of Applied Physics, 2015, 54, 08KC17.	1.5	0
196	Laser deposition for the controlled co-deposition of organolead halide perovskite. , 2016, , .		0
197	A XANES Study of Cu Valency in Cu-Doped Epitaxial ZnO. Physica Status Solidi (B): Basic Research, 2002, 229, 849-852.	1.5	0